Earth and Planetary Science Letters, 32 (1976) 25–34

[5]

SHEAR VELOCITY AND DENSITY OF AN ATTENUATING EARTH *

ROBERT S. HART, DON L. ANDERSON and HIROO KANAMORI

Seismological Laboratory, California Institute of Technology, Pasadena, Calif. 91125 (USA)

Received April 14, 1976
Revised version received June 14, 1976

The dispersion that must accompany absorption is taken into account in many recent body-wave investigations but has been largely ignored in surface-wave and free-oscillation studies. In order to compare body-wave and free-oscillation data a correction must be made to travel times or periods to account for absorption-related physical dispersion. The correction depends on the frequency and Q of the data and can be as high as 1% which is much larger than the uncertainty of the raw data. Corrected toroidal mode data is inverted to obtain shear velocity and density versus depth. The average shear velocity in the upper 600 km is ~2% greater than obtained from the uncorrected data. The resulting shear-wave travel times oscillate about the Jeffreys-Bullen values with an average baseline of only +0.5 second. Thus, the discrepancy between body-wave and free-oscillation studies is eliminated.

1. Introduction

Liu et al. [1] have recently re-examined the effect of attenuation on dispersion and have shown it to be of first order. Although negligible in some applications it becomes important when data over a wide frequency band are inverted for source and structure characteristics. The effect has also been studied by Futterman [2], Strick [3], Lomnitz [4] and Randall [5] and widely applied in body-wave studies [6]. Carpenter and Davies [7] and Davies [8] have attempted to correct for absorption in comparing body-wave and surface-wave models. Jeffreys [9,10] has also pointed out the need for an absorption correction.

The effect of absorption on free-oscillation periods has been ignored [11–15]. This is equivalent to assuming that the earth is a perfectly elastic body with frequency-independent elastic moduli. Discrepancies have been found with body-wave results [12,15] and these have been attributed to a "baseline" effect, a presumed difference between the "average earth" and that portion sampled by body-wave data, i.e. mostly continental receivers and mostly tectonic sources [12,16]. The magnitude of the difference between shear-wave travel times and those predicted from free-oscillation models, 4–6 seconds, led to the hypothesis that there must exist deep differences between continents and oceans [16]. Unlike such effects as rotation, ellipticity and lateral heterogeneity the effect of anelasticity results in a shift of all free-oscillation periods and it cannot be averaged out by accumulating more data.

The earth models produced by inversion of uncorrected normal mode data will yield lower velocities than models based on body-wave data [9] as Jeffreys has long maintained. It is imperative, then, that the problem of free-oscillation inversion be re-opened with the effects of attenuation being included. Based on the results of Liu et al. [1], we can compute the perturbation to the observed eigenperiods due to attenuation. We have applied the correction to observed toroidal more periods and have inverted to obtain the radial distribution of shear velocity and density in the earth. The resulting model provides an excellent fit to the normal mode data set, and also fits observed travel times without any baseline discrepancy.

* Contribution No. 2743, Division of Geological and Planetary Sciences, California Institute of Technology, Pasadena, California 91125.

2. Data and inversion

The detailed explanation of the Q correction is well covered by Liu et al. [1] and Anderson et al. [17] and will not be reiterated here. These authors, and others, have shown that elastic velocities are independent of frequency only at very high and very low frequencies or for a material of infinite Q. Seismic frequencies are in a broad absorption and observed attenuations are such that seismic velocities do not reflect purely elastic properties nor can they be assumed to be frequency independent. Briefly, all we can now achieve in earth modeling is to correct all the data to a common reference frequency. The resulting elastic constants and densities will then be those which characterize the medium at that particular frequency, with attenuation still present. While this procedure will not yield the elastic constants of an equivalent ideally elastic body, it does make all the seismic data consistent. Following Liu et al. [1] and Anderson et al. [17], the necessary correction term is:

$$\Delta T_i/T_i = -(\pi Q_i)^{-1} \ln(\omega_R/\omega_i) \quad (1)$$

where T_i is the period, Q_i^{-1} is the dissipation function and ω_i is the angular frequency, all referring to the ith mode, and ω_R is the angular reference frequency.

In our investigation, we have chosen ω_R to correspond to a period of 1 second. This is approximately the characteristic period of body-wave studies and thus allows us to directly compare the present normal mode results to body-wave studies. In this case, eq. 1 reduces to the form:

$$\Delta T_i/T_i = -(\pi Q_i)^{-1} \ln(T_i) \quad (2)$$

We assume that the intrinsic dissipation function of the medium, $\hat{Q}^{-1}$, is frequency independent and the observed variation of Q among the toroidal modes is due entirely to a variation of absorption with depth, as proposed by Anderson and Archambeau [18]. We do not dismiss the possibility of an intrinsic frequency dependence of $\hat{Q}$ over the seismic band but present data is not adequate to pursue this possibility further.

If the dissipation function, Q, is known for a particular mode, we can readily determine the required correction term. For many modes in the free-oscillation data set Q has been directly measured. Using these known Q's, we can construct a $\hat{Q}$ versus depth model and compute theoretical Q values for the entire data set. In particular, $\hat{Q}$ model MM8 [19] fits the observed toroidal data very closely. This model is tabulated in Table 1. MM8 is used to determine Q values and corrected periods for the 192 toroidal modes used in the inversion study of Anderson and Hart [15]. These data are from Dziewonski and Gilbert [11], Mendiguren [20], Gilbert and Dziewonski [13], Bolt and Currie [21] and Kanamori (unpublished results). Table 2 lists observed eigenperiods, errors, Q's, corrected periods and the model eigenperiods. Fig. 1 illustrates the percentage change in period for the fundamental mode and first five toroidal overtones.

TABLE 1

$\hat{Q}$ model MM8 *

Layer thickness (km)	Depth to top of layer (km)	$\hat{Q}_\mu$
38	0	450
22	38	60
10	60	80
55	70	100
375	125	150
100	500	180
100	600	250
100	700	450
100	800	500
100	900	600
1886	1000	750

* Anderson et al. [19].

The starting model for the present inversion was a modification of model C2 [15]. This model incorporates fine structure determined from studies of Helmberger and Wiggins [22], Helmberger and Engen [23],

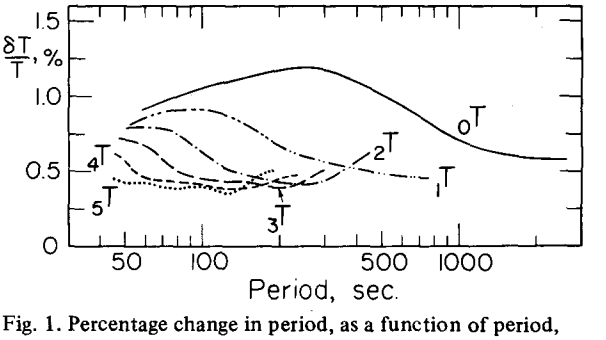

Fig. 1. Percentage change in period, as a function of period, for the fundamental toroidal modes and for the first five toroidal overtones.

TABLE 2

Computed and observed eigenperiods

Mode	Data (s)	Error (%)	Q	Corrected data (s)	QM1 (s)	Diff. (%)
${}_0T_2$	2636.38	0.08	428	2620.98	2617.93	0.12
${}_0T_3$	1702.51	0.15	392	1692.23	1693.61	−0.08
${}_0T_4$	1303.60	0.07	356	1295.24	1296.29	−0.08
${}_0T_5$	1075.20	0.09	323	1067.80	1068.88	−0.10
${}_0T_6$	925.36	0.09	295	918.54	919.28	−0.08
${}_0T_7$	817.92	0.08	271	811.48	812.04	−0.07
${}_0T_8$	736.86	0.05	252	730.72	730.58	0.02
${}_0T_9$	671.80	0.06	236	665.90	666.11	−0.03
${}_0T_{10}$	619.02	0.05	223	613.34	613.51	−0.03
${}_0T_{11}$	574.62	0.08	212	569.13	569.60	−0.08
${}_0T_{12}$	536.93	0.05	203	531.63	532.25	−0.11
${}_0T_{13}$	504.94	0.08	196	499.83	500.02	−0.04
${}_0T_{14}$	476.64	0.08	189	471.69	471.83	−0.03
${}_0T_{15}$	451.83	0.06	184	447.05	446.93	0.03
${}_0T_{16}$	429.50	0.07	179	424.87	424.73	0.03
${}_0T_{17}$	409.61	0.05	175	405.13	404.79	0.08
${}_0T_{18}$	391.16	0.10	171	386.81	386.76	0.01
${}_0T_{19}$	374.76	0.05	168	370.55	370.35	0.05
${}_0T_{20}$	359.59	0.08	165	355.51	355.35	0.05
${}_0T_{21}$	345.60	0.15	163	341.65	341.57	0.02
${}_0T_{22}$	332.75	0.13	161	328.93	328.82	0.03
${}_0T_{23}$	320.92	0.12	159	317.21	317.08	0.04
${}_0T_{24}$	310.00	0.14	157	306.39	306.15	0.08
${}_0T_{25}$	299.81	0.16	156	296.32	295.96	0.12
${}_0T_{26}$	290.12	0.15	154	286.72	286.44	0.10
${}_0T_{27}$	281.16	0.15	153	277.86	277.53	0.12
${}_0T_{28}$	272.70	0.15	152	269.50	269.16	0.13
${}_0T_{29}$	264.72	0.14	151	261.61	261.28	0.12
${}_0T_{30}$	257.19	0.14	150	254.16	253.86	0.12
${}_0T_{31}$	250.13	0.14	149	247.18	246.86	0.13
${}_0T_{32}$	243.65	0.23	149	240.79	240.23	0.23
${}_0T_{33}$	237.11	0.16	148	234.11	233.95	0.07
${}_0T_{34}$	231.06	0.17	147	228.34	227.99	0.16
${}_0T_{36}$	220.07	0.26	146	217.48	216.93	0.25
${}_0T_{37}$	214.33	0.22	146	211.82	211.80	0.01
${}_0T_{38}$	209.68	0.17	145	207.22	206.90	0.15
${}_0T_{39}$	204.65	0.17	145	202.25	202.23	0.01
${}_0T_{40}$	200.19	0.17	145	197.86	197.76	0.05
${}_0T_{41}$	195.94	0.14	144	193.65	193.48	0.09
${}_0T_{42}$	191.65	0.19	144	189.42	189.39	0.02
${}_0T_{43}$	187.73	0.19	144	185.55	185.46	0.05
${}_0T_{44}$	183.99	0.17	143	181.85	181.70	0.09
${}_0T_{45}$	180.38	0.15	143	178.29	178.08	0.12
${}_0T_{46}$	176.91	0.15	143	174.87	174.60	0.15
${}_1T_2$	756.57	0.08	465	753.14	752.95	0.03
${}_1T_3$	695.18	0.07	452	691.98	690.60	0.20
${}_1T_4$	629.98	0.10	441	627.05	626.78	0.04
${}_1T_6$	519.09	0.06	415	516.60	515.97	0.12
${}_1T_7$	475.17	0.13	399	472.84	472.24	0.13
${}_1T_8$	438.49	0.05	382	436.27	435.69	0.13

TABLE 2 (continued)

Mode	Data (s)	Error (%)	Q	Corrected data (s)	QM1 (s)	Diff. (%)
${}_1T_9$	407.73	0.10	367	405.61	405.11	0.12
${}_1T_{10}$	381.65	0.10	354	379.61	379.27	0.09
${}_1T_{11}$	359.14	0.05	343	375.18	357.08	0.03
${}_1T_{12}$	339.54	0.06	335	337.66	337.76	−0.03
${}_1T_{13}$	322.84	0.12	328	321.03	320.69	0.11
${}_1T_{16}$	280.59	0.06	311	278.97	279.35	−0.14
${}_1T_{20}$	240.98	0.09	288	239.52	239.51	0.00
${}_1T_{24}$	211.95	0.05	264	210.58	210.60	−0.01
${}_1T_{25}$	205.85	0.05	258	204.49	204.58	−0.04
${}_1T_{26}$	200.27	0.05	252	198.93	198.96	−0.01
${}_1T_{29}$	185.34	0.05	236	184.03	184.07	−0.02
${}_1T_{30}$	180.80	0.06	231	179.50	179.69	−0.11
${}_1T_{31}$	176.85	0.07	227	175.57	175.54	0.02
${}_1T_{33}$	169.27	0.05	218	168.00	167.91	0.05
${}_1T_{34}$	165.72	0.05	214	164.46	164.38	0.05
${}_1T_{35}$	162.36	0.05	210	161.11	161.03	0.05
${}_1T_{36}$	159.11	0.05	207	157.87	157.83	0.02
${}_1T_{37}$	156.08	0.05	203	154.84	154.79	0.03
${}_1T_{38}$	153.17	0.08	200	151.94	151.88	0.04
${}_1T_{39}$	150.28	0.07	197	149.06	149.09	−0.02
${}_1T_{40}$	147.68	0.05	195	146.48	146.43	0.04
${}_1T_{41}$	145.12	0.07	192	143.92	143.87	0.04
${}_1T_{42}$	142.66	0.06	190	141.47	141.41	0.04
${}_1T_{43}$	140.23	0.08	188	139.06	139.04	0.01
${}_1T_{44}$	137.96	0.06	186	136.80	136.77	0.02
${}_1T_{45}$	135.64	0.24	184	134.49	134.58	−0.06
${}_1T_{46}$	133.63	0.07	182	132.49	132.46	0.02
${}_1T_{47}$	131.59	0.17	180	130.45	130.42	0.02
${}_1T_{48}$	129.56	0.06	179	128.44	128.45	−0.01
${}_1T_{50}$	125.92	0.08	176	124.82	124.70	0.10
${}_1T_{51}$	124.13	0.43	174	123.04	122.91	0.11
${}_1T_{52}$	122.26	0.14	173	121.18	121.18	0.00
${}_1T_{54}$	118.96	0.13	171	117.90	117.86	0.03
${}_1T_{57}$	114.41	0.12	168	113.38	113.24	0.13
${}_1T_{58}$	112.92	0.12	167	111.90	111.78	0.11
${}_1T_{59}$	111.40	0.09	166	110.39	110.36	0.02
${}_1T_{60}$	110.24	0.13	165	109.24	108.98	0.23
${}_1T_{62}$	107.44	0.13	164	106.47	106.33	0.13
${}_1T_{64}$	104.94	0.13	163	103.99	103.81	0.18
${}_1T_{66}$	102.59	0.14	161	101.65	101.40	0.24
${}_2T_2$	447.30	0.09	311	444.50	444.53	−0.01
${}_2T_4$	419.38	0.09	322	416.87	417.09	−0.05
${}_2T_5$	401.82	0.09	332	399.50	399.67	−0.04
${}_2T_7$	363.65	0.07	360	361.76	361.11	0.18
${}_2T_8$	343.34	0.06	378	341.65	341.41	0.07
${}_2T_{17}$	219.95	0.06	402	219.01	218.94	0.03
${}_2T_{18}$	211.90	0.06	396	210.99	211.06	−0.03
${}_2T_{19}$	204.63	0.10	391	203.74	203.85	−0.05
${}_2T_{21}$	191.91	0.06	380	191.06	191.03	0.01
${}_2T_{22}$	186.19	0.06	374	185.36	185.30	0.03
${}_2T_{25}$	171.12	0.12	358	170.34	170.26	0.05

TABLE 2 (continued)

Mode	Data (s)	Error (%)	Q	Corrected data (s)	QM1 (s)	Diff. (%)
${}_2T_{26}$	166.50	0.07	353	165.73	165.85	−0.07
${}_2T_{27}$	162.58	0.09	348	161.82	161.68	0.09
${}_2T_{28}$	158.43	0.05	344	157.69	157.75	−0.03
${}_2T_{29}$	154.70	0.06	339	153.97	154.02	−0.03
${}_2T_{31}$	147.71	0.06	331	147.00	147.13	−0.09
${}_2T_{32}$	144.59	0.06	327	143.89	143.92	−0.02
${}_2T_{34}$	138.62	0.06	319	137.94	137.96	−0.02
${}_2T_{35}$	135.73	0.06	315	135.06	135.18	−0.09
${}_2T_{36}$	133.14	0.06	311	132.47	132.53	−0.04
${}_2T_{37}$	130.51	0.06	306	129.85	129.98	−0.10
${}_2T_{38}$	128.17	0.08	302	127.51	127.55	−0.03
${}_2T_{39}$	125.71	0.06	298	125.06	125.21	−0.12
${}_2T_{40}$	123.56	0.06	294	122.91	122.97	−0.05
${}_2T_{41}$	121.57	0.05	289	120.93	120.82	0.09
${}_2T_{42}$	119.33	0.14	285	118.69	118.76	−0.06
${}_2T_{44}$	115.49	0.06	276	114.86	114.88	−0.01
${}_2T_{45}$	113.57	0.06	271	112.94	113.04	−0.09
${}_2T_{47}$	110.22	0.06	262	109.59	109.58	0.01
${}_2T_{49}$	106.98	0.06	253	106.35	106.37	−0.02
${}_2T_{51}$	104.01	0.06	245	103.38	103.39	−0.01
${}_2T_{52}$	102.60	0.06	241	101.97	101.99	−0.02
${}_2T_{54}$	99.93	0.06	233	99.30	99.29	0.01
${}_2T_{55}$	98.61	0.06	230	97.98	98.01	−0.03
${}_2T_{58}$	95.08	0.06	220	94.45	94.42	0.03
${}_2T_{61}$	91.85	0.07	211	91.23	91.15	0.09
${}_3T_{9}$	259.26	0.12	395	258.10	258.01	0.03
${}_3T_{11}$	240.50	0.10	416	239.49	239.65	−0.07
${}_3T_{17}$	189.97	0.13	429	189.23	189.96	−0.39
${}_3T_{18}$	184.09	0.09	420	183.36	183.47	−0.06
${}_3T_{19}$	178.17	0.09	410	177.45	177.53	−0.04
${}_3T_{20}$	172.74	0.06	401	172.03	172.07	−0.02
${}_3T_{21}$	167.69	0.06	393	166.99	167.05	−0.03
${}_3T_{23}$	158.54	0.06	381	157.87	158.04	−0.11
${}_3T_{24}$	154.81	0.12	377	154.15	153.97	0.12
${}_3T_{25}$	150.66	0.05	374	150.02	105.13	−0.07
${}_3T_{29}$	137.24	0.07	366	136.65	136.71	−0.04
${}_3T_{33}$	126.16	0.06	361	125.62	125.65	−0.03
${}_3T_{34}$	123.75	0.06	359	123.22	123.18	0.03
${}_3T_{37}$	116.89	0.06	353	116.39	116.37	0.01
${}_3T_{41}$	108.87	0.06	343	108.40	108.49	−0.08
${}_3T_{47}$	99.08	0.06	325	98.63	98.67	−0.04
${}_3T_{51}$	93.67	0.09	315	93.24	93.14	0.10
${}_3T_{59}$	84.35	0.09	294	83.94	83.93	0.01
${}_3T_{65}$	78.69	0.10	276	78.29	78.26	0.04
${}_3T_{72}$	73.16	0.10	252	72.76	72.71	0.06
${}_4T_{7}$	216.81	0.18	369	215.80	216.04	−0.11
${}_4T_{11}$	199.74	0.19	374	198.84	198.99	−0.07
${}_4T_{14}$	184.86	0.19	383	184.06	184.46	−0.22
${}_4T_{16}$	174.72	0.19	393	173.99	174.46	−0.27
${}_4T_{20}$	155.64	0.19	414	155.04	155.12	−0.05
${}_4T_{22}$	147.47	0.19	416	146.91	146.57	0.23

TABLE 2 (continued)

Mode	Data (s)	Error (%)	Q	Corrected data (s)	QM1 (s)	Diff. (%)
${}_4T_{23}$	143.67	0.19	415	143.12	142.67	0.31
${}_4T_{25}$	136.30	0.20	412	135.78	135.59	0.14
${}_4T_{27}$	130.03	0.23	408	129.54	129.33	0.17
${}_4T_{40}$	101.27	0.30	356	100.85	100.93	−0.08
${}_4T_{45}$	93.79	0.10	340	93.39	93.48	−0.10
${}_4T_{48}$	89.82	0.10	334	89.43	89.57	−0.16
${}_4T_{50}$	87.46	0.09	331	87.08	87.16	−0.09
${}_4T_{54}$	82.95	0.10	327	82.59	82.73	−0.17
${}_4T_{63}$	74.72	0.09	317	74.40	74.33	0.10
${}_4T_{64}$	73.79	0.09	316	73.47	73.51	−0.05
${}_4T_{65}$	72.94	0.10	315	72.62	72.70	−0.11
${}_4T_{66}$	72.28	0.10	314	71.97	71.92	0.07
${}_5T_9$	174.33	0.10	339	173.48	173.57	−0.05
${}_5T_{10}$	171.84	0.08	341	171.06	171.11	−0.03
${}_5T_{15}$	157.57	0.10	364	156.87	156.82	0.03
${}_5T_{38}$	97.11	0.09	365	96.72	96.73	−0.01
${}_5T_{40}$	94.12	0.08	363	93.74	93.73	0.01
${}_5T_{44}$	88.64	0.09	364	88.29	88.30	−0.01
${}_5T_{45}$	87.47	0.09	364	87.13	87.04	0.10
${}_5T_{50}$	81.60	0.10	362	81.28	81.29	−0.01
${}_5T_{55}$	76.52	0.09	356	76.22	76.30	−0.11
${}_5T_{57}$	74.75	0.09	352	74.46	74.48	−0.03
${}_6T_{34}$	97.13	0.10	393	96.77	96.69	0.08
${}_6T_{35}$	95.46	0.09	392	95.11	95.05	0.06
${}_6T_{41}$	86.70	0.09	388	86.38	86.43	−0.05
${}_6T_{42}$	85.35	0.09	387	85.04	85.16	−0.14
${}_6T_{45}$	81.85	0.10	383	81.55	81.58	−0.03
${}_6T_{49}$	77.65	0.09	375	77.36	77.30	0.08
${}_6T_{53}$	73.89	0.09	366	73.61	73.52	0.13
${}_7T_8$	129.67	0.39	347	129.09	128.74	0.27
${}_7T_{17}$	118.57	0.13	346	118.05	118.14	−0.08
${}_7T_{19}$	115.58	0.14	347	115.08	115.24	−0.14
${}_7T_{28}$	101.15	0.13	376	100.75	101.00	−0.25
${}_7T_{29}$	99.53	0.13	384	99.15	99.33	−0.17
${}_7T_{30}$	97.93	0.13	392	97.58	97.65	−0.07
${}_7T_{34}$	91.46	0.14	417	91.14	91.06	0.09
${}_7T_{38}$	85.45	0.13	413	85.16	85.19	−0.03
${}_7T_{40}$	82.84	0.14	405	82.55	82.60	−0.06
${}_7T_{46}$	76.18	0.13	385	75.91	75.94	−0.04
${}_7T_{49}$	73.36	0.15	378	73.09	73.09	0.00

Hart [24], and Whitcomb [25]. It includes a 3-km ocean layer, a well-developed low-velocity zone for both P and S, and a first-order discontinuity at 670 km (to be consistent with the P'P' precursor data of Engdahl and Flinn [26] and Whitcomb and Anderson [27]). Model C2 represents an excellent fit to the uncorrected normal data set but disagrees, as do all recent inversion studies, with shear-wave travel times. The main effect of the inversion which led to model C2 was to decrease the velocities from 100 to 600 km from the body-wave starting model. Prior to the present inversion we smoothed C2 shear velocities below the

low-velocity zone and used a Bullen [28] Model A density profile down to a depth of about 400 km. The core radius was fixed at 3485 km, the value determined by Jordan and Anderson [12] and consistent with Engdahl and Johnson [29], Hales and Roberts [30] and Gilbert and Dziewonski [13].

The corrected data were inverted using the technique described by Jordan and Anderson [12]. The resulting model, designated QM1, fits the corrected toroidal data with an average error of 0.07%; 77% of the modes are fit to within one standard deviation and 97% to within two standard deviations (the 95% confidence interval).

The errors assigned to the "observed" periods are based entirely on the uncertainties of the data and do not include uncertainties in the Q correction. The correction term is uncertain by about 20%, considering the scatter in the Q data, and the errors assigned to the corrected data should be increased by about this amount, i.e. data assigned an error of 0.05% should probably be assigned an error of 0.06%. This small difference is unimportant for present purposes.

The inverted model is plotted in Fig. 2. The largest perturbation to the starting model is in the upper mantle. Fig. 3 shows the upper mantle shear velocity for the new model, QM1, plotted with model C2 for comparison. The change is almost a uniform increase in velocity throughout the region. In Table 3, we have tabulated the model parameters V_S and ρ for the crust and mantle. The core structure is identical to model C2 [15]. In Table 4 we compare the upper mantle

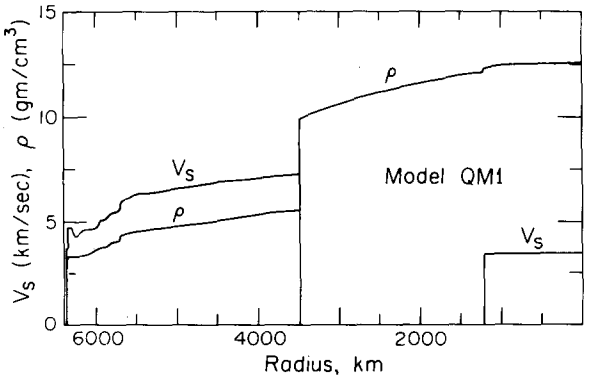

Fig. 2. Model QM1; V_S (shear velocity) and ρ (density) as a function of radius.

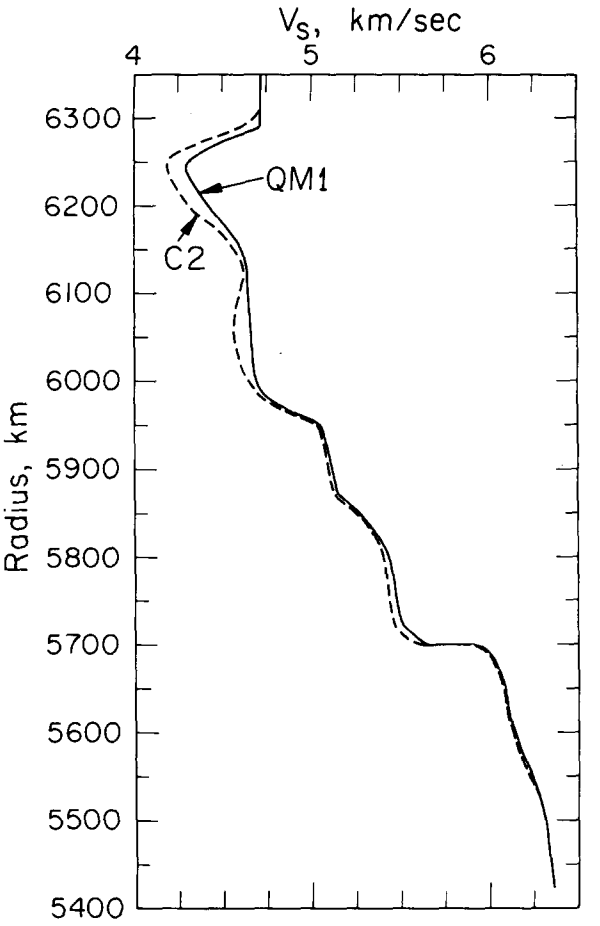

Fig. 3. Upper mantle shear velocity structure of model QM1 compared with that of model C2 [15].

shear velocities with other recent models. Model SHR14 is a body-wave model [23] of the western U.S. and C2 is a normal model based on uncorrected periods [15].

Earth models based on the inversion of normal mode data, uncorrected for absorption, give predicted shear-wave travel times that disagree with observations by 4–10 seconds [11–15]. This has been attributed to oceanic-continental discrepancy differences extending to great depths [16]. However, such rationalizations are no longer necessary. Table 5 lists the shear-wave travel times for model QM1 and Jeffreys-Bullen (J-B) times. In Fig. 4, we have plotted J-B residuals for

TABLE 3

Model QM1

Radius (km)	V_S (km/s)	ρ (g/cm^3)
6371	0.0	1.03
6368	0.0	1.03
6368	3.72	2.80
6350	3.72	2.80
6350	4.71	3.29
6330	4.73	3.30
6310	4.72	3.30
6290	4.73	3.31
6270	4.46	3.32
6250	4.29	3.32
6225	4.33	3.33
6200	4.42	3.34
6175	4.52	3.35
6150	4.60	3.36
6125	4.63	3.38
6100	4.64	3.41
6075	4.65	3.44
6050	4.65	3.50
6025	4.66	3.57
6000	4.68	3.63
5983	4.72	3.69
5967	4.87	3.70
5950	5.05	3.73
5925	5.08	3.76
5900	5.11	3.79
5875	5.13	3.80
5850	5.28	3.81
5825	5.37	3.95
5800	5.43	3.99
5775	5.46	4.00
5750	5.48	4.02
5725	5.50	4.04
5700	5.66	4.08
5700	5.91	4.35
5675	6.05	4.37
5660	6.07	4.39
5643	6.09	4.40
5625	6.10	4.42
5602	6.14	4.45
5573	6.18	4.49
5550	6.24	4.51
5500	6.32	4.54
5452	6.37	4.58
5350	6.38	4.61
5275	6.39	4.64
5200	6.46	4.68
5125	6.53	4.72
5050	6.57	4.75
4975	6.60	4.79
4900	6.64	4.82
4825	6.68	4.86

TABLE 3 (continued)

Radius (km)	V_S (km/s)	ρ (g/cm^3)
4750	6.73	4.90
4675	6.78	4.94
4600	6.83	4.98
4525	6.86	5.02
4450	6.90	5.06
4375	6.93	5.10
4300	6.96	5.15
4225	6.99	5.20
4150	7.02	5.25
4075	7.05	5.30
4000	7.08	5.35
3925	7.12	5.39
3850	7.15	5.44
3775	7.19	5.47
3700	7.22	5.49
3625	7.24	5.51
3550	7.25	5.54
3510	7.26	5.54
3485	7.26	5.55

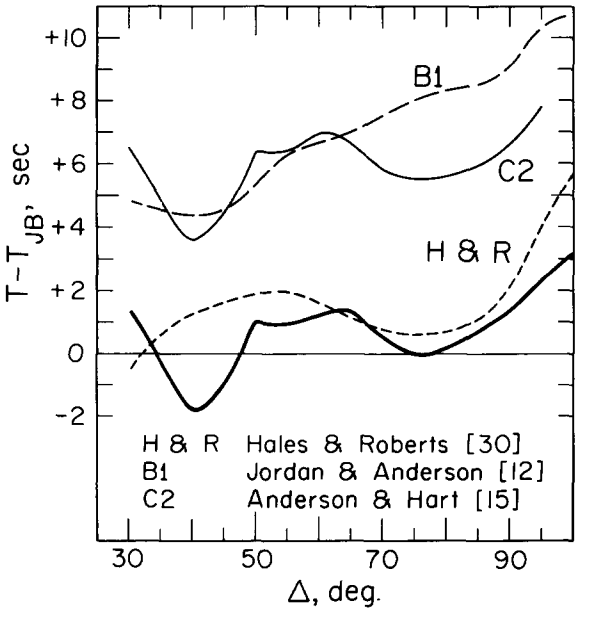

Fig. 4. Shear-wave travel-time residuals, relative to the Jeffreys-Bullen Tables [31], for model QM1, Hales and Roberts [30], model B1 [12] and model C2 [15].

TABLE 4

Upper mantle shear velocities

Radius (km)	SHR14 [23] (km/s)	C2 [15] (km/s)	QM1 (km/s)
6371	3.69	0.0	0.0
6368	3.69	0.0	0.0
6368	3.69	3.72	3.72
6350	3.69	3.72	3.72
6350	4.45	4.71	4.71
6330	4.45	4.73	4.73
6310	4.39	4.72	4.72
6290	4.32	4.62	4.73
6270	4.43	4.36	4.46
6250	4.44	4.18	4.29
6225	4.46	4.22	4.33
6200	4.48	4.30	4.42
6175	4.50	4.45	4.52
6150	4.52	4.57	4.60
6125	4.54	4.62	4.63
6100	4.56	4.59	4.64
6075	4.58	4.57	4.65
6050	4.62	4.57	4.65
6025	4.65	4.59	4.66
6000	4.72	4.64	4.68
5983	4.85	4.71	4.72
5967	4.98	4.86	4.87
5950	5.10	5.04	5.05
5925	5.16	5.07	5.08
5900	5.18	5.10	5.11
5875	5.22	5.12	5.13
5850	5.39	5.26	5.27
5825	5.43	5.34	5.37
5800	5.43	5.40	5.43
5775	5.47	5.42	5.46
5750	5.57	5.43	5.48
5725	5.75	5.45	5.50
5700	5.90	5.60	5.67

model QM1 and results from several other recent studies. The structure in the QM1 residual curve is consistent with Hales and Roberts [30] and Hart [24]. More importantly, the QM1 baseline shift is only +0.5 second. ScS-S differential times for deep-focus events are tabulated in Table 6. Model QM1 fits this data as well or better than previous models [12,15]. In short, there is no longer any discrepancy between free-oscillation and body-wave results.

TABLE 5

Shear-wave travel times (surface focus)

Δ (deg.)	Time (s)		QM1	dt/dΔ (s/deg.)	
	(1)	(2)		(2)	QM1
30	670.2	669.5	671.5	15.4	15.5
35	748.2	749.0	747.8	15.3	15.1
40	824.5	825.7	822.8	15.2	14.9
45	897.9	899.5	896.9	14.5	14.7
50	968.6	970.5	969.6	13.9	13.9
55	1036.8	1038.7	1037.8	13.4	13.4
60	1102.6	1104.1	1103.8	12.8	13.0
65	1165.5	1166.7	1166.8	12.2	12.1
70	1225.6	1226.4	1226.0	11.7	11.6
75	1282.6	1283.2	1282.6	11.1	11.1
80	1336.5	1337.3	1336.7	10.5	10.6
85	1387.3	1388.5	1388.0	10.0	9.9
90	1434.5	1436.9	1435.8	9.4	9.2
95	1478.2	1482.4	1480.6	8.8	8.8
100	1520.4		1523.6		8.4

(1) Jeffreys and Bullen [31].
(2) Hales and Roberts [30].

TABLE 6

ScS-S times (deep focus)

Δ (deg.)	Observed time * (s)	QM1 time (s)	Diff. (s)
30	311.3 ± 1.8	307.2	−4.1
35	259.4 ± 1.5	258.8	−0.6
40	215.7 ± 1.6	213.8	−1.9
45	174.3 ± 1.1	172.7	−1.6
50	138.6 ± 1.4	138.2	−0.4
55	108.6 ± 1.4	107.5	−1.0
60	82.0 ± 1.1	80.9	−1.1
65	59.7 ± 0.9	59.4	−0.3
70	40.6 ± 1.0	41.4	+0.8
75	25.5 ± 1.3	26.7	+1.2
80	14.0 ± 0.8	15.0	+1.1

* Jordan and Anderson [12]; uncertainty is 95% confidence interval.

3. Discussion and summary

Previous attempts to determine the structure of the earth from inversion of surface waves and free oscillations have ignored the important effect of dispersion due to absorption. The notable exceptions are Carpenter and Davies [7] and Davies [8]. Jeffreys

[10] has pointed out the importance of the effect. Liu et al. [1] derived the necessary correction term and also provided a physical basis for a nearly frequency-independent Q by superposition of relaxation peaks. The correction term is also implicit in the work of Futterman [2], Lomnitz [4] and Strick [3]. Jeffreys [9] based his conclusion that absorption was important on Lomnitz' Law [4]. Liu et al. [1] showed that the absorption-dispersion relation derived by the above authors is of general validity.

We have corrected the toroidal mode data set for absorption and have inverted to obtain a new gross earth shear velocity and density profile. The major change from previous inversion attempts is a substantially higher upper mantle shear velocity. The resulting model fits the toroidal eigenperiods with an average error of 0.07%. Moreover, the shear-wave travel times predicted by the model show only a +0.5 baseline shift relative to the Jeffreys-Bullen tables. The previous discrepancy between free-oscillation results and those due to body waves no longer exists. Hence, the present results do not require deep oceanic-continental mantle differences. The rather larger task of correcting the spheroidal mode data set for attenuation and adding those modes to the inversion is presently in progress. Preliminary results indicate very little, if any, change in the shear structure from model QM1. Compressional velocities in the upper mantle increase upon inversion of the corrected spheroidal mode data set.

The inversion of surface-wave data to obtain regional models of the upper mantle must also include the effects of absorption. Continental shield paths have higher phase velocities and lower attenuation than tectonic or oceanic paths. The corrected phase velocity data should show a smaller spread and this will also affect conclusions regarding upper mantle differences.

Acknowledgments

This research was supported by the Advanced Research Projects Agency of the Department of Defense and was monitored by the Air Force Office of Scientific Research under Contract F44620-72-C-0078. We would like to acknowledge helpful discussions with H.P. Liu and to credit M. Randall with reopening interest in this problem which has lain fallow in spite of the obvious implications of the work of Jeffreys, Futterman, Lomnitz, Strick, Davies and Carpenter.

References

1 H.-P. Liu, D.L. Anderson and H. Kanamori, submitted to Geophys. J. R. Astron. Soc. (1976).
2 W.I. Futterman, J. Geophys. Res. 67 (1962) 5279.
3 E. Strick, Geophys. J. R. Astron. Soc. 13 (1967) 197.
4 C. Lomnitz, J. Appl. Phys. 28 (1957) 201.
5 M.J. Randall, submitted to Phys. Earth Planet. Inter. (1976).
6 D.V. Helmberger, Geophys. J. R. Astron. Soc. 34 (1973) 251.
7 E.W. Carpenter and D. Davies, Nature 212 (1966) 134.
8 D. Davies, Geophys. J. R. Astron. Soc. 13 (1967) 421.
9 H. Jeffreys, Nature 208 (1965) 675.
10 H. Jeffreys, Geophys. J. R. Astron. Soc. 40 (1975) 23.
11 A. Dziewonski and F. Gilbert, Geophys. J. R. Astron. Soc. 27 (1972) 393.
12 T.H. Jordan and D.L. Anderson, Geophys. J. R. Astron. Soc. 36 (1974) 411.
13 F. Gilbert and A. Dziewonski, Philos. Trans. R. Soc. Lond., Ser. A, 278 (1975) 187.
14 A. Dziewonski, A.L. Hales and E.R. Lopwood, Phys. Earth Planet. Inter. 10 (1975) 12.
15 D.L. Anderson and R.S. Hart, J. Geophys. Res. 81 (1976) in press.
16 T.H. Jordan, Nature 257 (1975) 745.
17 D.L. Anderson, H. Kanamori, R.S. Hart and H.-P. Liu, submitted to Science (1976).
18 D.L. Anderson and C.B. Archambeau, J. Geophys. Res. 69 (1964) 2071.
19 D.L. Anderson, A. Ben-Menahem and C.B. Archambeau, J. Geophys. Res. 70 (1965) 1441.
20 J.A. Mendiguren, Geophys. J. R. Astron. Soc. 33 (1973) 281.
21 B.A. Bolt and R.G. Currie, Geophys. J. R. Astron. Soc. 40 (1975) 107.
22 D.V. Helmberger and R.A. Wiggins, J. Geophys. Res. 76 (1971) 3229.
23 D.V. Helmberger and G.R. Engen, J. Geophys. Res. 79 (1974) 4017.
24 R.S. Hart, J. Geophys. Res. 80 (1975) 4897.
25 J.H. Whitcomb, Part I, Ph. D. Theses, California Institute of Technology, Pasadena, Calif. (1973).
26 E.R. Engdahl and E.A. Flinn, Science 163 (1963) 177.
27 J.H. Whitcomb and D.L. Anderson, J. Geophys. Res. 75 (1970) 5713.
28 K.E. Bullen, Bull. Seismol. Soc. Am. 30 (1940) 235.
29 E.R. Engdahl and L.E. Johnson, Geophys. J. R. Astron. Soc. 39 (1974) 435.
30 A.L. Hales and J.L. Roberts, Bull. Seismol. Soc. Am. 60 (1970) 1427.
31 H. Jeffreys and K.E. Bullen, Seismological Tables (British Association for the Advancement of Science, Gray-Milne Trust, 1958).